tions were incubated with primary antibodies in PBS/2% Triton X-100 at 4 °C overnight. Antibodies against the following neuronal or glial marker proteins were used: neuron-specific nuclear protein (NeuN; mouse IgG, 1:500; Cat. No. MAB377, Millipore, Billerica, MA, USA), tyrosine hydroxylase (TH; mouse IgG, 1:1000; Cat. No. T2928, Sigma-Aldrich, St. Louis, MO, USA), glial fibrillary acidic protein (GFAP; rabbit IgG, 1:200; Cat. No. Z0334, Dako, Glostrup, Denmark), and oligodendrocyte transcription factor 2 (Olig2; rabbit IgG, 1:2000 Cat. No. AB9610, Millipore, Billerica, MA, USA). Following PBS rinses, the sections were incubated with secondary antibodies in PBS at 4 °C for 5 h. Secondary antibodies (Alexa goat anti-mouse 594 IgG [1:500; Cat. No. A11005, Molecular Probes, Eugene, OR, USA] or Alexa goat anti-rabbit 594 IgG [1:500; Cat. No. A11012, Molecular Probes, Eugene, OR, USA]), which were directed against the species in which the primary antibody was raised, were used in each case.

Imaging, cell quantification, and statistics

Brain sections were mounted on glass slides with Fluoromount-G (Beckman Coulter, Fullerton, CA, USA). Immunofluorescence and EGFP fluorescence were observed under a confocal laser-scanning microscope (LSM5 Pascal, Zeiss, Oberkochen, Germany) at a resolution of 1024×1024 pixels and one confocal plane. Co-expression of NeuN, GFAP, or Olig2 with EGFP-fluorescence was quantified using ImageJ software (National Institute of Health, Bethesda, MD, USA, http://rsb.info.nih.gov/ij/) with a 40× objective lens. For cell counting analyses, we examined 5–12 microscopic fields in two to four adjacent sections in each case. The number of EGFP-positive cells was statistically analyzed by the chi-square test using JMP8 (SAS Institute, Cary, NC, USA).

Viral transgene detection

Brain slices prepared as in the immunohistochemical analyses (see above) were used for the viral transgene detection assay. Small volumes of tissue were sampled from the injection sites and from regions that contained neuron populations expressing retrograde EGFP labels, under the guidance of EGFP fluorescence by microscopic observation. Extraction and polymerase chain reaction (PCR) amplification of total DNA were performed using the KAPA MG Kit (Cat. No. KK7153, Kapa Biosystems, Woburn, MA, USA). Viral transgenes were detected by PCR using the EGFP (5′-TATATCATGGCCGACAAGCA-3′) and WPRE (5′-CCACATAGCGTAAAAGGAGCA-3′) primers. For internal controls, β-actin DNA was amplified using the primers for β-actin 001 (5′-TCCTGACCCTGAAGTACCCC-3′) and β-actin 002 (5′-GTGGTGGTGAAGCTGTAGCC-3′) (Sasaki et al., 2009).

Thirty-five cycles of PCR were performed (15 s each at 95, 62, and 72 °C) in between an initial denaturation at 95 °C for 3 min and a final elongation at 72 °C for 10 min. PCR products were analyzed by electrophoresis on a 1.2% agarose gel.

RESULTS

Preferential neuronal tropism of AAV9 in marmoset and macaque brains

We have previously shown that AAV8 exhibits a strong tropism for neurons, but not for glia, in the marmoset brain (Masamizu et al., 2010). The present study aimed to determine the tropism of AAV9, which is another promising neurotropic serotype, in the marmoset brain. Recombinant AAV9 expressing the EGFP gene under the CAG promoter (AAV9-EGFP) was generated and stereotaxically injected into the striatum of two marmoset monkeys (Fig. 1A). Four weeks after injection, striatal sections were observed with a confocal microscope. EGFP fluorescence was visible in numerous cell bodies and processes around the injection site (Fig. 1B). Immunohistochemistry revealed that almost all EGFP-positive cells also expressed NeuN (Fig. 1D). Computer-aided cell counting revealed that 99% of EGFP-positive cells also expressed NeuN (Table 2). In contrast, co-expression of EGFP-positive cells with the astrocyte marker GFAP or the oligodendrocyte marker Olig2 was rarely detected (Fig. 1E, F, Table 2). Frequencies of co-localization of cell type-specific markers with EGFP signals were significantly different across cell types ($P<0.0001$, chi-square test; Table 2). Because CAG promoter activity was expected to be ubiquitous across neuronal and glial cell types, these results indicate strong endogenous neuronal tropism of AAV9.

AAV9 neurotropism was also observed in the macaque monkey, the most widely used primate model animal in neuroscience research. AAV9-EGFP was injected into the primary visual cortex of two macaque monkeys. EGFP fluorescence was coexpressed almost exclusively with NeuN, but rarely with glial markers (Fig. 2).

Viral gene transfers to neuronal pathways after the striatum infection

To date, AAV8 and AAV9 infection patterns (local infection from cell bodies/dendrites or retrograde infection from axon terminals) in primate brains have not been elucidated; however, the reciprocal projections between the striatum and substantia nigra offer an appropriate model system for analyzing this. GABAergic neurons in the striatum project to the substantia nigra pars reticulata (SNr), and dopaminergic neurons in the substantia nigra pars compacta (SNc) project to the striatum (Albin et al., 1989; Alexander and Crutcher, 1990; Minamimoto et al., 2009) (Fig. 3B). Therefore, either AAV8-EGFP or AAV9-EGFP was injected into the marmoset striatum, followed by analysis of EGFP expression in the SNr and SNc, ipsilateral to the injection side (Fig. 3A). For both vectors, strong EGFP fluorescence was directly observed in axon terminals in the SNr, as well as in cell bodies of the SNc (Fig. 3C, F). Almost all EGFP-positive cells in the SNc were dopaminergic neurons, as revealed by co-expression of TH (Fig. 3D, G), indicating retrograde EGFP gene transfers after the viral infection in the striatum. We counted the number of EGFP-positive cells among TH-positive neurons to estimate efficacy of retrograde gene transfers. Proportions of EGFP-positive cells among TH-positive neurons were 38% for AAV8 (EGFP-positive/TH-positive: 81/216), and 49% for AAV9 (EGFP-positive/TH-positive: 102/208). In the SNr, high-power confocal images revealed EGFP-positive fibers and varicosities surrounding NeuN-positive cell bodies (Fig. 3E, H). These results suggested that an AAV8-EGFP or AAV9-EGFP injection into the striatum resulted in anterograde transport of transgene products to nerve terminals in the SNr via the striatonigral pathway, as well as retrograde transport of the transgene to cell bodies in the SNc via the nigrostriatal dopaminergic pathway (Fig. 3B).

The striatum receives major projections from the thalamus and the cerebral cortex (Alexander and Crutcher,

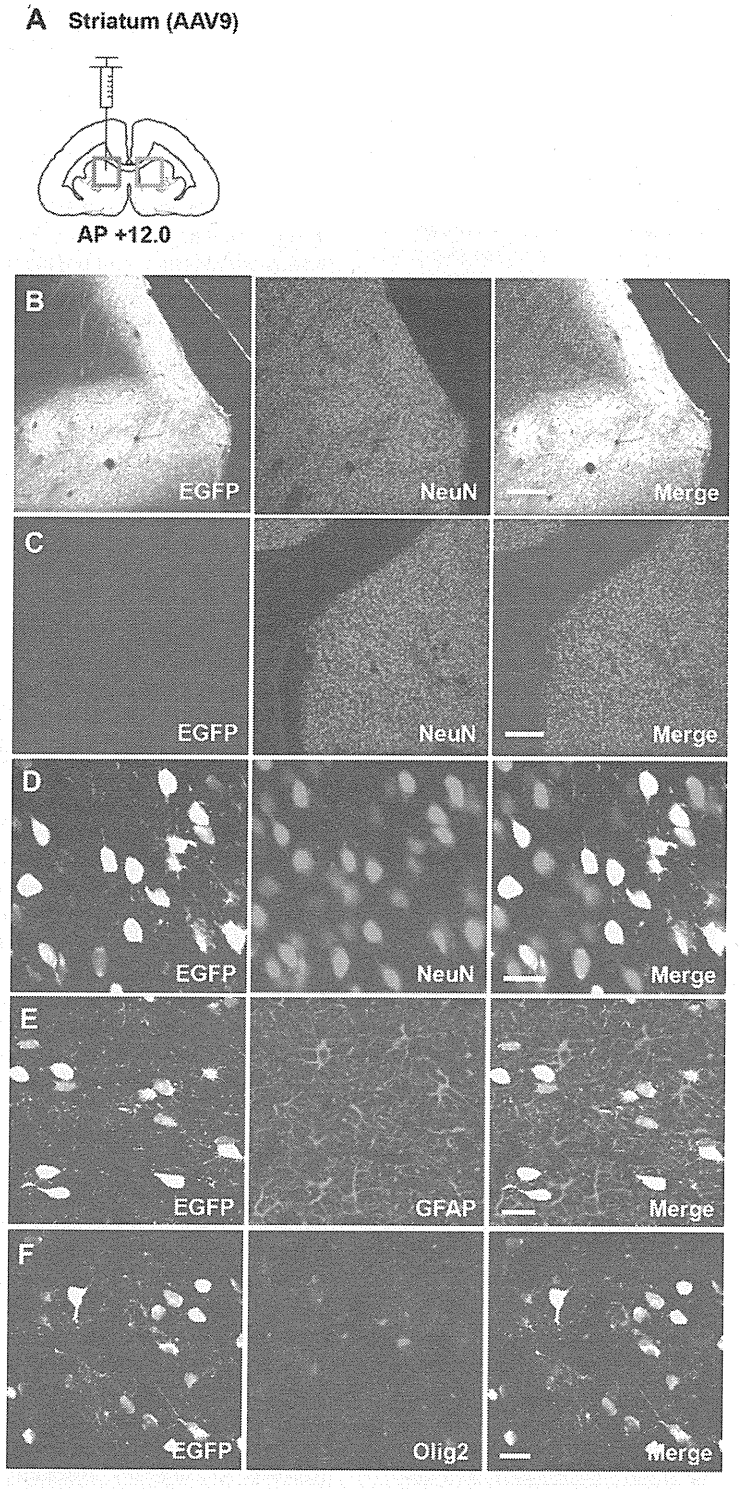

Fig. 1. Efficient gene transfer into neurons of the marmoset striatum using AAV9. (A) The striatal injection site is indicated on a coronal section of the marmoset brain, approximately 12 mm anterior to the interaural line. (B) Low power confocal images corresponding to the red box on the coronal marmoset brain map in (A). Native EGFP fluorescence (left, green), NeuN immunofluorescence signal (center, red), and the merged image (right) are shown. (C) Images of the noninjected control side corresponding to the light-blue box in (A). (D) Confocal images of high-power fields reveal that EGFP-positive cells (green) co-express NeuN (red), as shown by the merged image (yellow). (E, F) EGFP-positive cells (green) rarely co-express GFAP (E; red) or Olig2 (F; red). Bars=200 μm in (B, C) and 20 μm in (D–F). AAV9, adeno-associated virus serotype 9; AP, anteroposterior; EGFP, enhanced green fluorescent protein; GFAP, glial fibrillary acidic protein; NeuN, neuron-specific nuclear protein; Olig2, oligodendrocyte transcription factor 2.

Table 2. Proportion of cells expressing NeuN, GFAP, or Olig2 in EGFP-positive cells in the striatum and primary visual cortex of marmosets following AAV8-EGFP or AAV9-EGFP viral injection

Injection site	Neuron ($NeuN^+/EGFP^+$ cells)	Astrocyte ($GFAP^+/EGFP^+$ cells)	Oligodendrocyte ($Olig2^+/EGFP^+$ cells)
Striatum (AAV8)	98% (484/494)	0% (0/497)	1% (5/500)
Striatum (AAV9)	99% (492/495)	0% (0/500)	1% (3/497)
Primary visual cortex (AAV8)	99% (490/497)	0% (0/502)	1% (3/498)
Primary visual cortex (AAV9)	98% (494/505)	0% (0/493)	1% (5/502)

In all cases, the frequencies of colocalization of cell type-specific markers with EGFP signals are significantly different across cell types ($P<0.0001$, chi-square-test).

1990; Minamimoto et al., 2009). Thus, we also sought retrogradely infected neurons in these regions. We found EGFP expressing neuronal somata in the thalamus probably corresponding to the parafascicular thalamic nucleus (Fig. 4B) (Minamimoto et al., 2009; Yuasa et al., 2010). Neurons expressing EGFP were also found in the frontal and insular cortices at almost the same anterior–posterior level as the striatal injection site (Fig. 4C, D) (Yuasa et al., 2010).

To further confirm retrograde neuronal infections by AAV8 and AAV9, we aimed to detect AAV transgenes in neurons with retrograde EGFP labels. We extracted total DNA from small areas of the frontal/insular cortices and the thalamus where retrograde EGFP labels were observed, and performed PCR using the primers complimentary to a sequence within the AAV construct. For both AAV8 and AAV9, we detected the presence of viral transgenes in the frontal/insular cortices and in the thalamus (Fig. 4E), indicating the viral transgene itself was transported to remote somata after retrograde infections with AAV8 or AAV9.

Local and retrograde gene transfer to the geniculocortical pathway

Gene transfer capabilities of AAV8 and AAV9 were subsequently analyzed in the marmoset visual system. The primary visual cortex (V1) and lateral geniculate nucleus (LGN) constitute reciprocal loops typical for corticothalamic pathways: feedforward projections from the LGN to V1 and feedback projections from the V1 to LGN (Felleman and Van Essen, 1991; Murphy and Sillito, 1996). Either AAV8-EGFP or AAV9-EGFP were injected into the marmoset V1, aiming at the region representing foveal retinotopy, according to previously described electrophysiological mappings (Fritsches and Rosa, 1996). Following injection, EGFP signals were observed across cortical layers at the injection site, and AAV8 and AAV9 neuronal tropisms were confirmed by nearly complete co-expression with NeuN (Table 2). EGFP fluorescence was then detected in the ipsilateral LGN (Fig. 5 for AAV9-EGFP; data not shown for AAV8-EGFP), demonstrating that V1 injection of either AAV8-EGFP or AAV9-EGFP resulted in EGFP expression in the LGN, which was in apparent retinotopic correspondence with the V1 injection site (White et al., 1998) (Fig. 5B). The EGFP labels were apparently restricted to the parvocellular layer (White et al., 1998). In confocal images with high-power magnification, EGFP-positive axons and varicosities were clearly identified (Fig. 5D), suggesting anterograde transport of the transgene products (EGFP) via projections from the V1 to LGN. Neuronal somata also expressed EGFP in the LGN, suggesting retrograde axonal transport of the transgene from the V1 injection site (Fig. 5D). Efficacy of retrograde infections in the LGN were relatively low compared with that in the SNc. Proportions of EGFP-positive cells among NeuN-positive neurons were 15% for AAV8 (EGFP-positive/NeuN-positive: 26/170) and 22% for AAV9 (EGFP-positive/NeuN-positive: 38/173).

DISCUSSION

The present study demonstrated that AAV9 efficiently and selectively infected neurons *in vivo* in the marmoset brain (Fig. 1). This neuronal tropism was similar to that of AAV8, which was shown in our previous study (Masamizu et al., 2010). Results from the present study, in combination with our preliminary results, demonstrate strong AAV8 and AAV9 neurotropism in the brains of macaque monkeys, the most widely used primate animal model in neuroscience research (Fig. 2 for AAV9, data not shown for AAV8). These results suggest that AAV8 and AAV9 exhibit a wide range of neuronal infection across primate species, possibly including humans. To obtain selective transgene expression in neurons, neuron-specific promoters, such as the CaMKII promoter, are used typically. However, neuron-specific promoter activity is often weak and insufficient for effective transgene expression. Endogenous AAV8 and AAV9 tropisms permit efficient and almost exclusive neuronal transgene expression through the use of ubiquitous, strong promoters, such as the CAG promoter, rather than specific, weak promoters.

Recently, Foust et al. (2009, 2010) reported that intravascular injection of AAV9 allows transduction of neurons throughout the brain in newborn mice, as well as in spinal motoneurons of newborn cynomolgus monkeys. In adult mice, however, i.v. delivery of AAV9 results in preferential transduction of astrocytes, rather than neurons. In the present study, AAV9 infected, almost exclusively, neurons in the adult marmoset and macaque brain via direct virus injection into the parenchyma. The discrepancy in cell tropism may be attributed to species differences and/or differences in brain entry: i.v. vs. parenchyma injection. The structure of genomes and the purification procedure of viral particles may also affect cell tropism of AAV vectors. Here, we used conventional single-stranded AAV9 purified with ion-exchange chromatography, whereas Foust et al. used double-stranded, self-complementary AAV9 purified

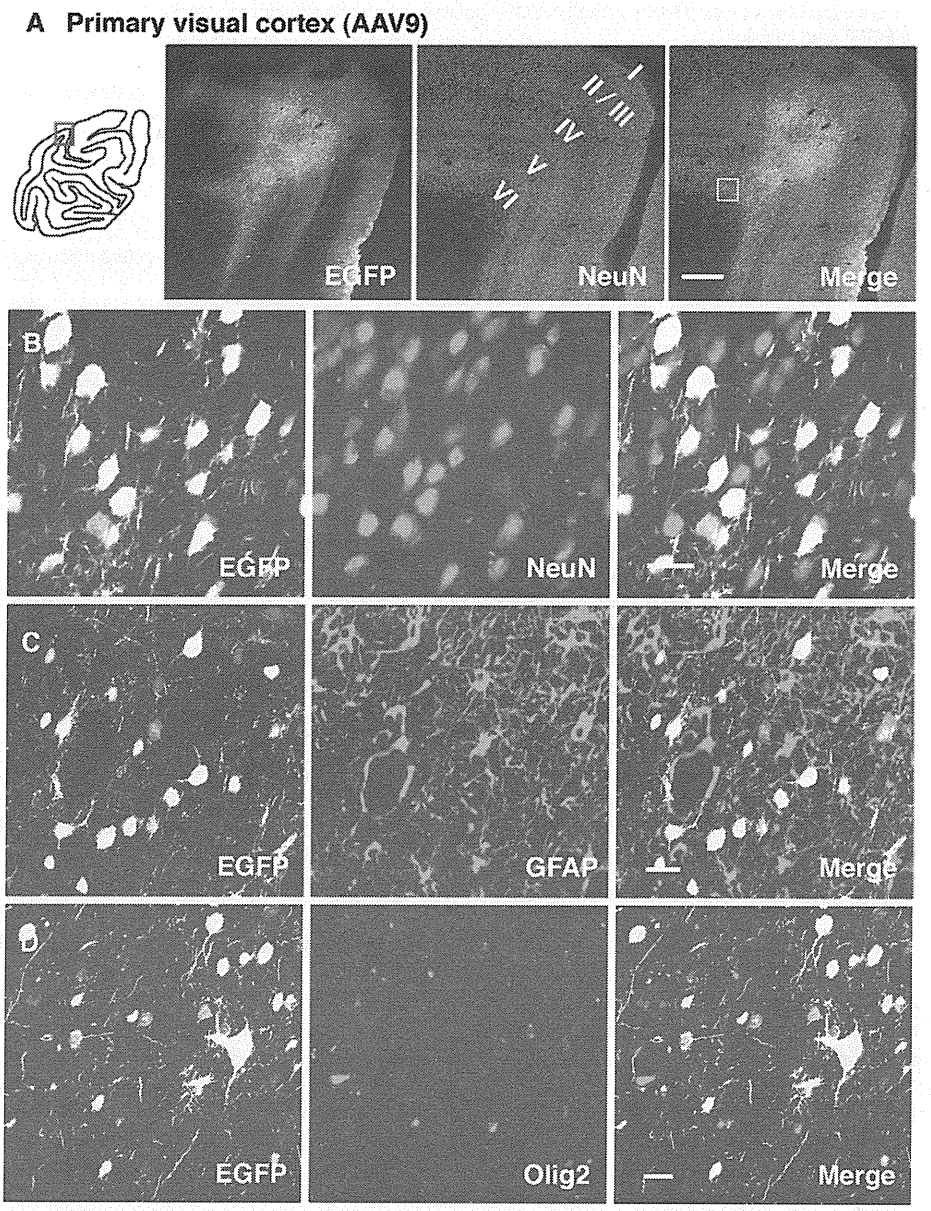

Fig. 2. Gene transfer into neurons of the primary visual cortex of macaque monkeys with AAV9. (A) Low power confocal images at the injection site, approximately corresponding to the red box on a coronal section of the macaque brain map (left). The confocal images reveal prominent EGFP fluorescence around the injection site (green) and NeuN signals (red). (B) Confocal images reveal co-expression of EGFP (green) and NeuN (red), as shown by the merged image (yellow). The view field approximately corresponds to the yellow box on the right panel of (A). (C, D) EGFP-positive cells rarely co-express GFAP (red) or Olig2 (red), as shown by the merged images. Bars=500 μm in (A) and 20 μm in (B–D). The abbreviations are as listed in Fig. 1.

without the use of ion-exchange chromatography. More importantly, results from Foust et al. demonstrated that AAV9 crossed the blood–brain barrier in mice and cynomolgus monkeys, which offers a method for brain-wide gene delivery with less invasiveness, especially for gene therapy applications.

The present study revealed, for the first time, neuronal infection patterns of AAV8 and AAV9 in the primate brain. AAV8, as well as AAV9, exhibited both local and retrograde infection patterns in nigrostriatal, corticostriatal, thalamostriatal and geniculocortical pathways. In the LGN, EGFP labeling was apparently restricted to the parvocellular layers. This observation, together with the observation of a lack of retrograde labeling in other brain regions, which are known to have connections with V1, may suggest that retrograde gene transfer after injection of AAV8 or AAV9 into the V1 are limited to the parvocellular layers of the LGN, although future experiments are required to obtain concrete evidence. For both AAV8 and AAV9, the number of neurons expressing EGFP by retrograde trans-

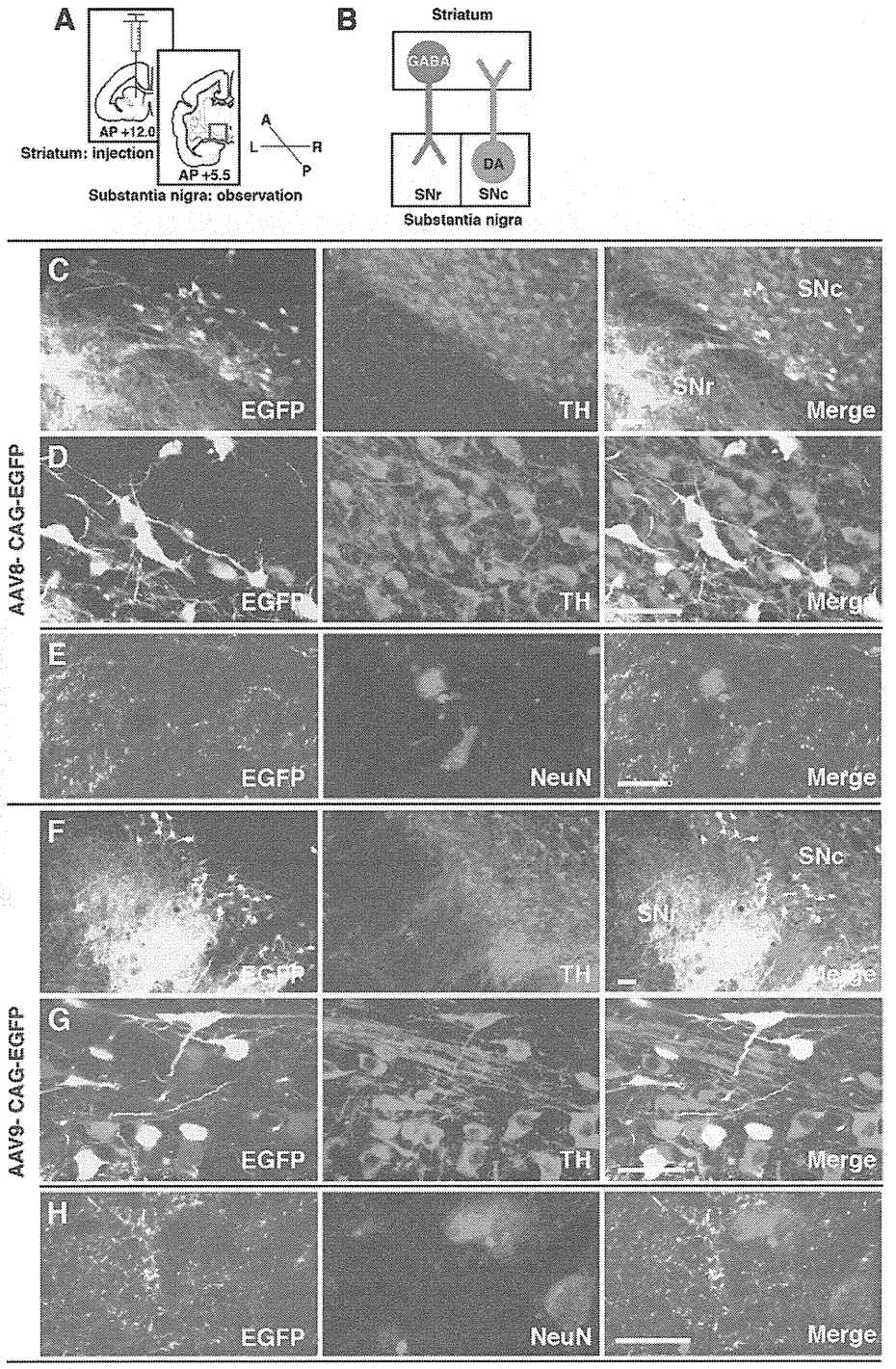

Fig. 3. Local and retrograde gene transfer into the marmoset nigrostriatal pathway with AAV8 and AAV9. (A) Experimental design. EGFP fluorescence is detected in the substantia nigra (red box) following AAV8-EGFP or AAV9-EGFP injection into the striatum. A, anterior; P, posterior; R, right; L, left. (B) Schematic diagram of the nigrostriatal pathway. GABAergic neurons in the striatum (GABA, blue) project to the SNr, and dopaminergic neurons (DA, orange) in the SNc project to the striatum. (C, F) EGFP fluorescence is observed in axon terminals in the SNr, as well as in cell bodies of the SNc following AAV8 (C) or AAV9 (F) injection. (D, G) High-power images of the SNc. EGFP-positive cell bodies (green) co-express TH (red), as shown by the merged images (yellow). (E, H) High-power images of the SNr. EGFP-positive fibers and varicosities (green) are evident around NeuN-positive cell bodies (red). Bars=50 μm in (C, D, F, G) and 20 μm in (E, H). AAV8, adeno-associated virus serotype 8; DA, dopamine; GABA, gamma-aminobutyric acid; SNc, substantia nigra pars compacta; SNr, substantia nigra pars reticulata; TH, tyrosine hydroxylase. Other abbreviations are as listed in Fig. 1.

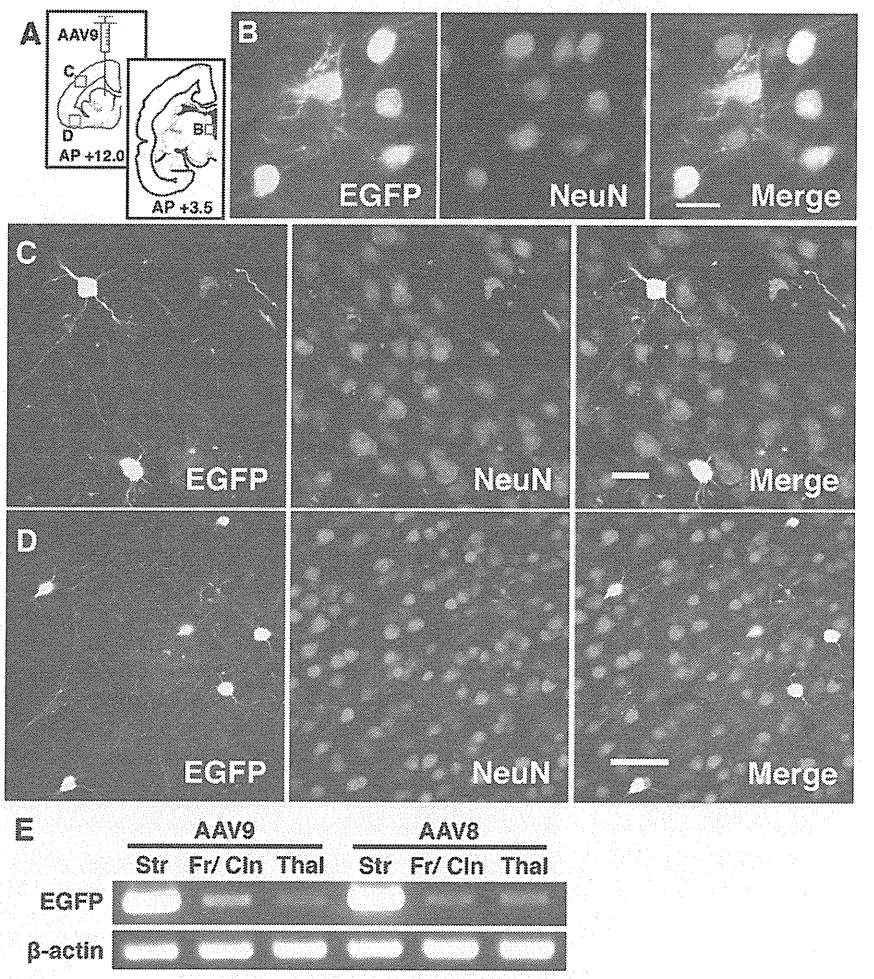

Fig. 4. Retrograde gene transfer into neurons of the frontal/insular cortices and thalamus following AAV9 injection into the striatum. (A) AAV9-EGFP was injected into the striatum at anteroposterior (AP) +12 mm. Retrograde EGFP labels were detected in the thalamus, probably corresponding to the parafascicular thalamic nucleus (B), the frontal cortex (C), and the insular cortex (D). (B–D) Confocal images indicate co-expression of EGFP (green) and NeuN (red) in the thalamus (B), the frontal cortex (C), and the insular cortex (D), as shown in the merged images (yellow). (E) Polymerase chain reaction (PCR) analyses reveal the presence of viral transgene (EGFP) not only in the striatal local infection site (Str), but also in the frontal/insular cortices (Fr/Cln) and the thalamus (Thal) in which cell bodies with retrograde EGFP fluorescence were observed. Bars=20 μm in (B, C) and 50 μm in (D). PCR, polymerase chain reaction. Other abbreviations are as listed in Fig. 1.

fer was modest in the substantia nigra and relatively small in the LGN. Transgene expression was examined at 4 weeks after viral injection; however, the time frame may be insufficient for acquiring full transgene expression in the somata via retrograde transport. In general, AAV-mediated transgene expression persists for long periods (more than a year), and long-term expression would allow for improved efficiency of neuronal transgene expression via retrograde AAV transport.

In the present study, we conducted PCR analyses and confirmed the presence of viral transgenes in the neuronal somata following retrograde infections of either AAV8 or AAV9. These results prove that the genome of AAV8 or AAV9 itself is transported to the soma after retrograde infection at the axon terminal in the brain. This probable mechanism has been demonstrated in several other AAV serotypes, such as AAV1, AAV2, and AAV6 (Kaspar et al., 2002; Hollis et al., 2008; Towne et al., 2010).

A number of neuroscience studies have demonstrated the roles of hierarchical and interconnected structures of the brain in terms of information processing for cognition and behavior (Felleman and Van Essen, 1991; Murphy and Sillito, 1996; Nishimura et al., 2007; Bostan et al., 2010). Retrograde neuronal delivery of molecular tools through the use of AAV8 or AAV9 vectors could provide methods for analyzing hierarchical information processing in the brain. For example, injection of recombinant AAV8 or AAV9 expressing transgenes encoding optogenetic tools into a given brain region could lead to transgene neuronal delivery with direct projections to the injected site, thereby allowing for experimental *in vivo* manipulation of neuronal inputs to the injected brain area. Therefore, transgene

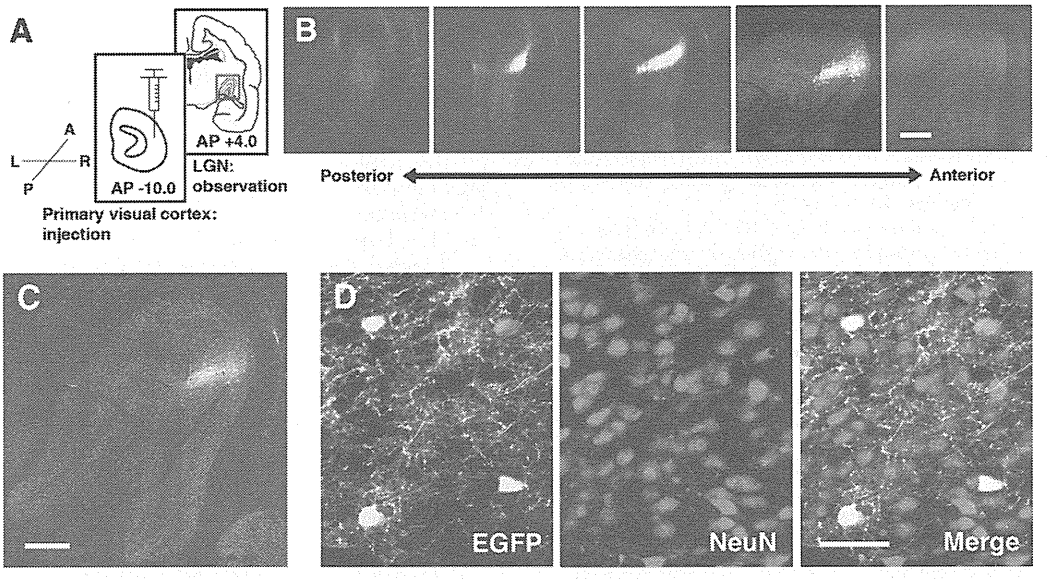

Fig. 5. Local and retrograde gene transfer into the marmoset geniculocortical pathway with AAV9. (A) Experimental design. EGFP expression is visible in the LGN (red box) following injection of AAV9-EGFP into the primary visual cortex. (B) Confocal images of EGFP fluorescence (green) and NeuN expression (red) in coronal sections of the LGN, approximately 3.4–4.2 mm anterior to the interaural line. (C) Representative coronal section of the LGN around the center of EGFP expression (green) overlaid on NeuN signals (red). Approximately 4.0 mm anterior to the interaural line. (D) High-power confocal images show EGFP-positive cell bodies, axons and varicosities (green) in the LGN. EGFP-positive cell bodies co-express NeuN (red), as shown by the merged image (yellow). Bars=500 μm in (B, C) and 50 μm in (D). LGN, lateral geniculate nucleus. Remaining abbreviations are as listed in Fig. 1.

delivery into primate brains via AAV8 and AAV9 vectors could facilitate studies focused on circuit-based principles of brain function by utilizing high-infection efficiencies, as well as neuronal infection patterns.

CONCLUSIONS

Results from the present study, in combination with our previous study, revealed that AAV8 and AAV9 exhibited strong endogenous tropism for neurons in primate brains. The present results further demonstrated that these AAV serotypes can infect neurons both locally and retrogradely. These infection patterns allow transgene delivery to local neurons surrounding virus-injection sites via local infection from somata/dendrites, as well as to distal neurons that project to virus-injection sites via retrograde infections from axon terminals.

Acknowledgments—We thank Dr. James M. Wilson for providing helper plasmids pAAV2-8 (originally described as p5E18-VD2/8) and pAAV2-9. This study was supported by the JSPS Research Fellowship for Young Scientists (Y.M.) and by PRESTO, JST (K.N.). All authors declare no conflict of interest.

REFERENCES

Albin RL, Young AB, Penney JB (1989) The functional anatomy of basal ganglia disorders. Trends Neurosci 12:366–375.

Alexander GE, Crutcher MD (1990) Functional architecture of basal ganglia circuits: neural substrates of parallel processing. Trends Neurosci 13:266–271.

Bostan AC, Dum RP, Strick PL (2010) The basal ganglia communicate with the cerebellum. Proc Natl Acad Sci U S A 107:8452–8456.

Broekman ML, Comer LA, Hyman BT, Sena-Esteves M (2006) Adeno-associated virus vectors serotyped with AAV8 capsid are more efficient than AAV-1 or -2 serotypes for widespread gene delivery to the neonatal mouse brain. Neuroscience 138: 501–510.

Chan AW, Chong KY, Martinovich C, Simerly C, Schatten G (2001) Transgenic monkeys produced by retroviral gene transfer into mature oocytes. Science 291:309–312.

Dodiya HB, Bjorklund T, Stansell J, III, Mandel RJ, Kirik D, Kordower JH (2010) Differential transduction following basal ganglia administration of distinct pseudotyped AAV capsid serotypes in nonhuman primates. Mol Ther 18:579–587.

Eslamboli A, Georgievska B, Ridley RM, Baker HF, Muzyczka N, Burger C, Mandel RJ, Annett L, Kirik D (2005) Continuous low-level glial cell line-derived neurotrophic factor delivery using recombinant adeno-associated viral vectors provides neuroprotection and induces behavioral recovery in a primate model of Parkinson's disease. J Neurosci 25:769–777.

Felleman DJ, Van Essen DC (1991) Distributed hierarchical processing in the primate cerebral cortex. Cereb Cortex 1:1–47.

Foust KD, Nurre E, Montgomery CL, Hernandez A, Chan CM, Kaspar BK (2009) Intravascular AAV9 preferentially targets neonatal neurons and adult astrocytes. Nat Biotechnol 27:59–65.

Foust KD, Wang X, McGovern VL, Braun L, Bevan AK, Haidet AM, Le TT, Morales PR, Rich MM Burghes AH, Kaspar BK (2010) Rescue of the spinal muscular atrophy phenotype in a mouse model by early postnatal delivery of SMN. Nat Biotechnol 28:271–274.

Fritsches KA, Rosa MG (1996) Visuotopic organisation of striate cortex in the marmoset monkey (Callithrix jacchus). J Comp Neurol 372:264–282.

Gao G, Vandenberghe LH, Alvira MR, Lu Y, Calcedo R, Zhou X, Wilson JM (2004) Clades of Adeno-associated viruses are widely disseminated in human tissues. J Virol 78:6381–6388.

Gao GP, Alvira MR, Wang L, Calcedo R, Johnston J, Wilson JM (2002) Novel adeno-associated viruses from rhesus monkeys

as vectors for human gene therapy. Proc Natl Acad Sci U S A 99:11854–11859.

Han X, Qian X, Bernstein JG, Zhou HH, Franzesi GT, Stern P, Bronson RT, Graybiel AM, Desimone R, Boyden ES (2009) Millisecond-timescale optical control of neural dynamics in the nonhuman primate brain. Neuron 62:191–198.

Hollis ER, II, Kadoya K, Hirsch M, Samulski RJ, Tuszynski MH (2008) Efficient retrograde neuronal transduction utilizing self-complementary AAV1. Mol Ther 16:296–301.

Kaplitt MG, Leone P, Samulski RJ, Xiao X, Pfaff DW, O'Malley KL, During MJ (1994) Long-term gene expression and phenotypic correction using adeno-associated virus vectors in the mammalian brain. Nat Genet 8:148–154.

Kaspar BK, Erickson D, Schaffer D, Hinh L, Gage FH, Peterson DA (2002) Targeted retrograde gene delivery for neuronal protection. Mol Ther 5:50–56.

Masamizu Y, Okada T, Ishibashi H, Takeda S, Yuasa S, Nakahara K (2010) Efficient gene transfer into neurons in monkey brain by adeno-associated virus 8. Neuroreport 21:447–451.

Matsushita T, Elliger S, Elliger C, Podsakoff G, Villarreal L, Kurtzman GJ, Iwaki Y, Colosi P (1998) Adeno-associated virus vectors can be efficiently produced without helper virus. Gene Ther 5:938–945.

Minamimoto T, Hori Y, Kimura M (2009) Roles of the thalamic CM-PF complex-Basal ganglia circuit in externally driven rebias of action. Brain Res Bull 78:75–79.

Murphy PC, Sillito AM (1996) Functional morphology of the feedback pathway from area 17 of the cat visual cortex to the lateral geniculate nucleus. J Neurosci 16:1180–1192.

Nakahara K, Adachi Y, Osada T, Miyashita Y (2007) Exploring the neural basis of cognition: multi-modal links between human fMRI and macaque neurophysiology. Trends Cogn Sci 11:84–92.

Nakahira E, Yuasa S (2005) Neuronal generation, migration, and differentiation in the mouse hippocampal primoridium as revealed by enhanced green fluorescent protein gene transfer by means of in utero electroporation. J Comp Neurol 483:329–340.

Nishimura Y, Onoe H, Morichika Y, Perfiliev S, Tsukada H, Isa T (2007) Time-dependent central compensatory mechanisms of finger dexterity after spinal cord injury. Science 318:1150–1155.

Okada T, Nomoto T, Yoshioka T, Nonaka-Sarukawa M, Ito T, Ogura T, Iwata-Okada M, Uchibori R, Shimazaki K, Mizukami H, Kume A, Ozawa K (2005) Large-scale production of recombinant viruses by use of a large culture vessel with active gassing. Hum Gene Ther 16:1212–1218.

Okada T, Nonaka-Sarukawa M, Uchibori R, Kinoshita K, Hayashita-Kinoh H, Nitahara-Kasahara Y, Takeda S, Ozawa K (2009) Scalable purification of adeno-associated virus serotype 1 (AAV1) and AAV8 vectors, using dual ion-exchange adsorptive membranes. Hum Gene Ther 20:1013–1021.

Okada T, Shimazaki K, Nomoto T, Matsushita T, Mizukami H, Urabe M, Hanazono Y, Kume A, Tobita K, Ozawa K, Kawai N (2002) Adeno-associated viral vector-mediated gene therapy of ischemia-induced neuronal death. Methods Enzymol 346:378–393.

Passingham R (2009) How good is the macaque monkey model of the human brain? Curr Opin Neurobiol 19:6–11.

Sasaki E, Suemizu H, Shimada A, Hanazawa K, Oiwa R, Kamioka M, Tomioka I, Sotomaru Y, Hirakawa R, Eto T, Shiozawa S, Maeda T, Ito M, Ito R, Kito C, Yagihashi C, Kawai K, Miyoshi H, Tanioka Y, Tamaoki N, Habu S, Okano H, Nomura T (2009) Generation of transgenic non-human primates with germline transmission. Nature 459:523–527.

Tan EM, Yamaguchi Y, Horwitz GD, Gosgnach S, Lein ES, Goulding M, Albright TD, Callaway EM (2006) Selective and quickly reversible inactivation of mammalian neurons in vivo using the Drosophila allatostatin receptor. Neuron 51:157–170.

Taymans JM, Vandenberghe LH, Haute CV, Thiry I, Deroose CM, Mortelmans L, Wilson JM, Debyser Z, Baekelandt V (2007) Comparative analysis of adeno-associated viral vector serotypes 1, 2, 5, 7, and 8 in mouse brain. Hum Gene Ther 18:195–206.

Towne C, Schneider BL, Kieran D, Redmond DE, Jr, Aebischer P (2010) Efficient transduction of non-human primate motor neurons after intramuscular delivery of recombinant AAV serotype 6. Gene Ther 17:141–146.

White AJ, Wilder HD, Goodchild AK, Sefton AJ, Martin PR (1998) Segregation of receptive field properties in the lateral geniculate nucleus of a New-World monkey, the marmoset Callithrix jacchus. J Neurophysiol 80:2063–2076.

Yasuda T, Miyachi S, Kitagawa R, Wada K, Nihira T, Ren YR, Hirai Y, Ageyama N, Terao K, Shimada T, Takada M, Mizuno Y, Mochizuki H (2007) Neuronal specificity of alpha-synuclein toxicity and effect of Parkin co-expression in primates. Neuroscience 144:743–753.

Yuasa S, Nakamura K, Kohsaka S (2010) Stereotaxic atlas of the marmoset brain with immunohistochemical architecture and MRI Images. National Institute of Neuroscience, National Center of Neurology and Psychiatry, Tokyo, Japan.

Zhang F, Wang LP, Brauner M, Liewald JF, Kay K, Watzke N, Wood PG, Bamberg E, Nagel G, Gottschalk A, Deisseroth K (2007) Multimodal fast optical interrogation of neural circuitry. Nature 446:633–639.

(Accepted 28 June 2011)
(Available online 18 July 2011)